Review Paper

ISSN 1225-6153
Online ISSN 2287-8955

Experimental Studies on Submerged Arc Welding Process

Degala Ventaka Kiran* and Suck-Joo Na*,†

*Department of Mechanical Engineering, KAIST, Daejeon 305-701, Korea

†Corresponding author : sjoona@kaist.ac.kr

(Received June 2, 2014 ; Revised June 17, 2014 ; Accepted June 18, 2018)

Abstract

The efficient application of any welding process depends on the understanding of associated process parameters influence on the weld quality. The weld quality includes the weld bead dimensions, temperature distribution, metallurgical phases and the mechanical properties. A detailed review on the experimental and numerical approaches to understand the parametric influence of a single wire submerged arc welding (SAW) and multi-wire SAW processes on the final weld quality is reported in two parts. The first part deals with the experimental approaches which explain the parametric influence on the weld bead dimensions, metallurgical phases and the mechanical properties of the SAW weldment. Furthermore, the studies related to statistical modeling of the present welding process are also discussed. The second part deals with the numerical approaches which focus on the conduction based, and heat transfer and fluid flow analysis based studies in the present welding process. The present paper is the first part.

Key Words : Submerged arc welding process, Statistical modeling, Weld bead dimensions, Metallurgical phases, Mechanical properties

1. Introduction

Demand of advanced joining methods with high productivity is ever increasing in ship building and other fabrication industries. Submerged arc welding (SAW) is traditionally considered as an efficient and highly productive joining technology for medium to high thickness steels[1]. In SAW process, the welding arc is always covered with a layer of granular flux that protects the arc [Fig. 1]. The flux melts by arc heating forming a slag that protects the weld pool from the atmosphere[1]. The final weld quality depends on the proper selection of the welding conditions. Weld quality includes the weld bead dimensions, temperature distribution, metall- urgical phases generated in the weld pool and the heat affected zone (HAZ), and mechanical properties of the weldment. The welding conditions involved in the SAW process include welding current and voltage, polarity, electrode extension and diameter, welding speed and type of the granular flux.

In pursuit towards enhancing the productivity of the conventional SAW process, increase in both welding current and welding speed are considered as possible recourses. However, higher welding current often results in undercut, humped bead and severe joint distortion[1,2-6,7]. Alternately, greater welding speed increases the propensity for defects such as centerline cracking and incomplete penetration[1,8-9,7]. Multi-wire SAW process can lead to a significant enhancement in welding productivity in comparison to the conventional SAW process, in particular, towards joining of medium to high thickness plates. However the increase of the number of wires increases the associated process parameters tremendously. This poses severe difficulty in the proper selection of the welding conditions. A quantitative understanding of the influence

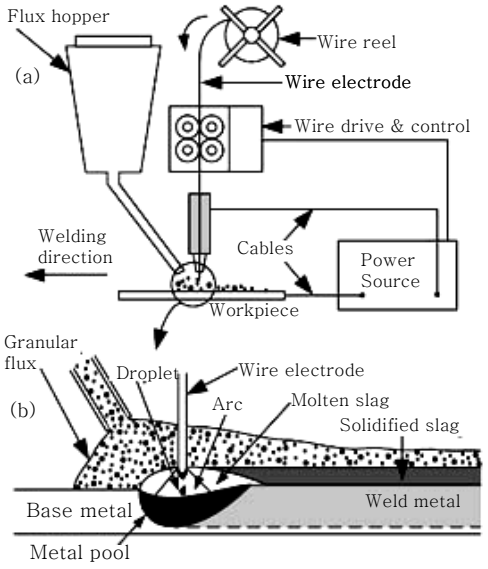

Fig. 1 Schematic representation of submerged arc welding process[1)]

of the process variables on the weld quality is challenging while essential for the successful application of the SAW and multi-wire SAW processes.

A detailed study on the influence of SAW process parameters on the final weld quality by various experimental techniques is performed till date by many researchers. Similar kind of studies in case of multi-wire SAW process is recently evolving. In this paper, a comprehensive literature review on the experimental routes to understand the SAW and multi-wire SAW process parameters influence on the weld bead dimensions, weldment metallurgical phases and mechanical properties are presented.

2. Experimental studies

2.1 Variants of SAW process

The multi-wire SAW variants include twin-wire and multi-wire / multi-power SAW processes [1-5)]. The twin-wire SAW process involves two small diameter wires fed through a single contact tube and controlled by a single power source. Hence the current from a single power source splits between the two wires equally. Increase in the current density in small diameter electrode and the interaction between the arcs increases the rate of deposition in a twin wire SAW process over a single wire SAW process for a given set of welding conditions[8)]. The twin-wire SAW process finds applications where higher deposition rates without attendant deep penetration are advantageous. These include surface depositions, heavy corner welds and various butt and fillet welds where avoidance of melt-through is crucial[8)].

The multi-wire SAW process consists of two or more wires controlled by separate power sources to produce a single elongated weld puddle. Each electrode is fed into the workpiece by its own separate feeder. However, the adjacent arcs are affected by strong interacting electromagnetic forces leading to deflection of the arc at high current levels and arc blow[1,8)]. The arc interaction can be controlled using DC-AC in place of DC-DC power source configuration. In general, the leading wire is set at higher currents to provide greater penetration while the trailing wire is set to lower current levels with an aim to control the weld shape[8,9)]. Furthermore, replacing the conventional AC power by pulsed AC power source for the trailing arc facilitates precise control on the arc heat input to achieve an improved bead profile[10)]. The high depositions associated with this process leads to its application in heavy industries like marine industries, pipe and pressure vessel manufacturing.

2.2 Influence of process parameters on weld quality

Welding current and voltage, polarity, welding speed, wire electrode diameter, electrode extension and its inclination with the weld seam significantly influence the electrode and flux melting rate, the final weld bead dimensions and weld joint properties in SAW process. Robinson et al.[2)] studied the influence of welding current and its polarity on the melting rate of the electrode and flux in single wire conventional SAW process. The authors observed increase in melting rate of the electrode and flux with increase in welding current. Furthermore, the electrode melting rate

is the highest in DCEN, followed by AC and DCEP for a given welding current. The flux melting rate is the highest in AC polarity followed by DCEN and DCEP at higher levels of welding current. The authors argued that greater electrode tip surface temperature resulted in larger droplets followed by higher melting rate of electrode and flux in DCEN in comparison to DCEP. Decrease in arc voltage has increased the electrode melting rate but decreased the flux melting rate. Smaller arc voltage reduces the arc length and thus, increases the electrode extension and its resistive heating resulting in greater rate of electrode melting. The smaller arc length, however, reduces the melting rate of flux.

Chande[3] investigated the influence of process variables on the electrode melting rate during SAW of 19 mm thick ASTM A36 steel plate. The author has observed that the electrode melting rate is inversely proportional to electrode diameter while increased directly with the increase in electrode extension. Smaller electrode diameter has resulted in greater current density and hence, higher electrode melting rate. In contrast, longer extension of the electrode tends to increase the preheating of the electrode due to joule effect resulting in greater melting rate of electrode and flux.

Renwick et al.[4] investigated the influence of welding current and electrode diameter on weld bead dimensions in SAW of 38 mm thick BS 4360 grade 43A mild steel plates. The authors reported that the weld penetration and reinforcement height increased with increase in welding current and decrease in electrode wire diameter. Murugan et al.[5] investigated the influence of welding voltage, welding speed, electrode extension, and wire feed rate on the weld bead dimensions in SAW of 20 mm thick IS 2062 steel plate. It was reported that the weld width, penetration and reinforcement height increased inversely with the welding speed and directly with the wire feed rate. Increase in welding voltage has decreased the reinforcement height and increased the weld width while showed no effect on the weld penetration. Increase in electrode extension has resulted in larger weld width and smaller penetration.

Tusek et al.[11] reported the influence of welding current, current polarity, electrode extension and diameter on the melting rate of the electrode in twin-wire SAW process and compared the same with single wire SAW process. The authors reported higher electrode melting rate in the case of the twin-wire SAW process in comparison to the same in single wire SAW process for a given welding current. In a subsequent work, greater electrode melting rate with a three-wire SAW process could be achieved by the same authors[12]. Konkol et al.[13] reported an extensive study on two-wire tandem SAW of 16.5 mm thick API Grade X-60 steel plates. At smaller welding current and shorter electrode extension length, increase in the inclination angle of the trailing electrode wire has decreased the weld penetration.

Grong et al.[14] presented a critical review on the classification of the weld microstructure developed in mild and HSLA steels during SAW processes. The authors reported that the final weld microstructure would depend on the cooling rate from 800 to 500℃ ($\Delta T_{8/5}$), prior austenite grain size, distribution of non-metallic inclusions and chemical composition of the weld. In particular, $\Delta T_{8/5}$ is envisaged to be an effective indicator of the extent of austenite to ferrite transformation in HSLA welds[14]. Babu et al.[15] presented an overview of the high temperature phase changes that would be expected in steel welds [Fig. 2] as function of melting and solidification, gas dissolution, and solid-state transformations. At high peak temperature, the liquid steel would dissolve oxygen. During cooling of the weld in the temperature range of 2000 to 1700℃, the dissolved oxygen and deoxidizing elements in liquid steel would react to form complex oxide inclusions in the range of 0.1 to 1.0 ㎛ [Fig. 2(a)]. Solidification of δ-ferrite would start in the temperature range 1700 to 1600℃ with δ-ferrite transforming to austenite [Fig. 2(b)]. In the temperature range 1600 to 800℃, austenite grain growth might

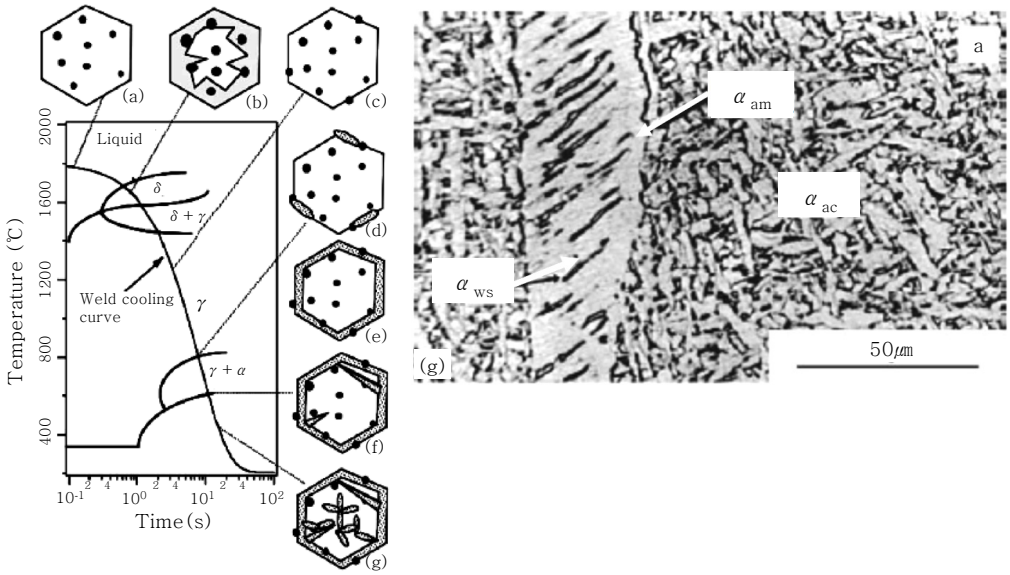

Fig. 2 Schematic illustrations of a weld metal cooling curve and a hypothetical continuous cooling transformation (CCT) diagrams showing different phase transformation that may occur as weld metal cools to room temperature[14,15]

occur [Fig. 2(c)]. The austenite would further decompose to different ferrite morphologies in the temperature range 800 to 500℃ forming allotriomorphic ferrite (α_{am}) at the prior γ-γ boundaries and eventual coverage of these boundaries [Figs. 2(d) and (e)]. With further cooling, the Widmanstatten (α_{ws}) ferrite would nucleate at the α/γ boundaries and extend into the untransformed austenite grain interiors [Fig. 2(f)]. Subsequently, the acicular ferrite (α_{ac}) would nucleate on the inclusion. If there are no potent inclusions, bainitic (α_b) ferrite might form instead of acicular ferrite from the remaining austenite. On further cooling to temperatures close to room temperature, any remaining austenite might completely or partially transform to martensite. This mixture of martensite-austenite phases is referred to as M-A constituent. Figure 2(g) depicts a typical weld microstructure having all the above mentioned phases.

Farrar et al.[16] reported a critical review on the influence of cooling rate $\Delta T_{8/5}$ on the volume fraction of acicular ferrite phase in carbon-manganese weld metals. The authors opined that the weld metal tensile strength and toughness would improve with greater volume fraction of acicular ferrite due to its fine grains, interlocking nature and high angle boundaries that could act as obstacles to cleavage crack propagation [15]. It was reported that the acicular ferrite would form in the intermediate transformation temperature range (650 to 500℃). The author also noted that increase in the cooling rate $\Delta T_{8/5}$ would lower the transformation temperature and increases the volume fraction of the acicular ferrite. Motohashi et al.[17] reported the influence of heat input on the final microstructure and the mechanical properties of C-Mn steel welds. The authors reported that the increase in the heat input has reduced hardness, yield strength and the ultimate tensile strength while enhanced the percentage elongation. The authors opined that increase in the heat input would decrease the volume fraction of acicular ferrite phase and increase the allotriomorphic and Widmanstatten ferrites leading to the degradation of weld mechanical properties. Bhadeshia et al.1[8] studied the influence of acicular ferrite on the Charpy impact toughness of SAW joints. It is reported that the increase in acicular ferrite phase in the weld pool would enhance the weld joint Charpy impact toughness.

Prasad et al.[19] investigated the influence of the SAW process parameters on the mechanical properties of HSLA steel welds. The weld joints were prepared at different heat inputs between

3.0 to 6.3 kJ/mm by varying welding currents and speeds from 500 to 700 A and from 200 to 300 mm/min, respectively. With the increase in heat input, the Charpy impact toughness has reached a peak value and then decreased with further increase in the heat input. Hashemi et al.[20] investigated the microstructure and mechanical properties of fusion zone, HAZ and base metal regions in SAW of C-Mn steel. The authors have observed greater hardness in the weld fusion zone in comparison to the same in the HAZ. However, the Charpy impact toughness was the highest in the base metal and the lowest in the fusion zone. The author attributed the greater fusion zone hardness to the presence of bainite and widmanstatten ferrite in the fusion zone microstructure. The lesser Charpy impact toughness value of fusion zone was attributed to the presence of the cast microstructure and of the allotriomorphic ferrite phases in the fusion zone microstructure. Hall[21] investigated the influence of welding speed on the mechanical properties of ASME SA516 Grade 70 steel SAW joints. The author has reported that increase in welding speed has increased the hardness and Charpy impact toughness values in both HAZ and weld metal. Increase in welding speed reduced the grain size in HAZ and fusion zone and the amount of allotriomorphic ferrite in the weld microstructure while increased the proportion of acicular ferrite.

Farhat et al.[22] investigated the effect of the process parameters during SAW of X80 steel. The welding was performed using single and two wires at different welding speeds (16.93, 19.69, 25.4, 29.63 and 33.87 mm/s). The authors have observed that increase in welding speed has resulted in excellent mechanical properties within the ranges considered in the experimental study. The tensile strength was improved and DBTT (ductile to brittle transition temperature) for the weld metal was shifted to lower temperatures. Viano et al.[23] investigated the influence of welding speed and the overall heat input on the weld profile, microstructure and mechanical properties in two-wire tandem submerged arc welds of HSLA steel. Increase in the welding speed at all heat inputs has produced weld profiles without any undercuts. Increase in the heat input has decreased the density of the inclusion and increased the average inclusion size. For a given welding speed, increase in heat input has decreased the acicular ferrite volume fraction, hardness and the Charpy impact toughness of the weld.

Moeinifar et al.[24,25] studied the influence of thermal cycles on the microstructure and the mechanical properties of the coarse grained heat affected zone (CGHAZ) in X80 microalloyed steel through simulated weld thermal cycles using Gleeble apparatus. The martensite-austenite constituents were observed in the HAZ for all the specimens along the prior-austenite grain boundaries. The hardness and toughness of CGHAZ increased with decrease in prior austenitic grain size and increase in the cooling rate ($\Delta T_{8/5}$). Kiran et al.[26] performed a detailed experimental investigation on the effect of five significant welding conditions on the weld bead quality in single-pass two wire tandem submerged arc welding (SAW-T) process of a typical HSLA steel. These welding conditions include leading arc current (I_{LE}), trailing arc positive current pulse (I^{+}_{TR}), trailing arc negative current pulse (I^{-}_{TR}), trailing arc negative current pulse duration (t^{-}_{TR}) and welding speed (v). Figures 3(a-f) show the effect of SAW-T welding conditions on the measured weld bead profile. A comparison

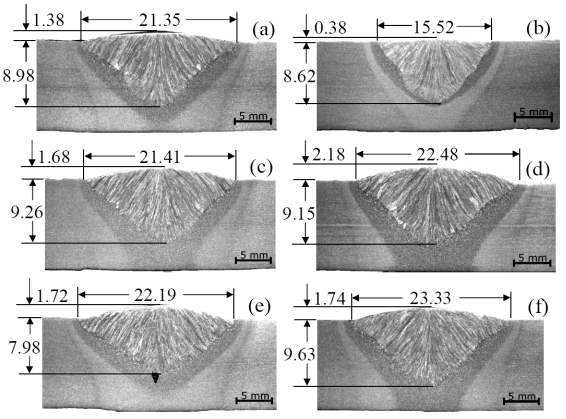

Fig. 3 Influence of SAW-T process parameters on weld bead dimensions[26]

of Figs. 3(a) and (b) depict a decrease in the weld bead dimensions with increase in welding speed (v) from 10.0 to 14.45 mm/s for a constant other parameters. Increase in welding speed reduces the rate of heat input leading to smaller weld bead dimensions. In contrast, increase in either trailing wire negative current pulse (I_{TR}^{-}) from 563 to 797 A [Figs. 3(c) and (d)] or in leading wire current (I_{LE}) from 384 to 507 A [Figs. 3(e) and (f)] for a constant other parameter results in higher weld bead dimensions. Increase in trailing wire current pulses and leading wire current results in higher rate of heat input and greater weld bead dimensions. Kiran et al.[26] also observed that the leading and trailing arc currents have negative influence while the trailing wire negative pulse time and welding speed have positive influence on the acicular ferrite volume fraction and the weld mechanical properties. Similar trend of volume fractions were also observed in some other works (14, 16, 27, 28). In typical tandem submerged arc welding of HSLA steel, welding speed from 9.0 to 11.5 mm/s, leading wire current from 530 to 580 A, and trailing wire negative current from 680 to 910 A are found to be the most suitable[29].

The leading and trailing arcs attract during a like-polarity condition of the welding current and repel under unlike polarities, referred to as arc interaction. Arc interaction has a significant influence on the stability of the arc, and there is a possibility that it can also influence the leading and trailing arc root dimensions. The arc root dimensions include the effective front and rear arc length from its center in the welding direction as well as the effective transverse length[35]. This variation in the arc interaction and root dimensions with the welding condition can affect the arc energy distribution on the work plate and subsequently the final weld quality. Hence, the successful application of the SAW-T process strongly requires a detailed investigation of the effect of the welding condition on the arc interaction, and the leading and trailing arc root dimensions.

Kiran et al.[30] made an attempt to determine the arc behavior in the SAW-T process for a wide range of leading and trailing arc welding conditions. It was observed that the magnitude of the leading arc center displacement is less when compared to the trailing arc for same current values. Next, based on the Biot-Savart law and the spring model [Fig. 4] the leading and trailing arc physical models are formulated as

$$x_L^P = -4.0\left(\frac{I_T}{I_L}\right)\left(\frac{l_L^2}{d}\right)\left[\sin\left(\phi_1^T\right)+\sin\left(\phi_2^T\right)\right] \quad (1)$$

$$x_T^P = 2.75\left(\frac{I_L}{I_T}\right)\left(\frac{l_T^2}{d}\right)\left[\sin\left(\phi_1^L\right)+\sin\left(\phi_2^L\right)\right] \quad (2)$$

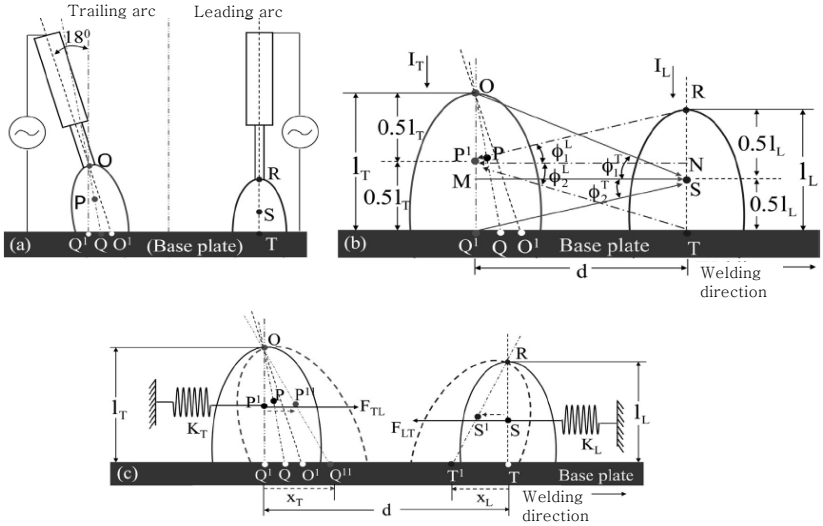

Fig. 4 Schematic representation of theoretical interaction between leading and trailing arcs[30]

The estimated arc center displacements were compared with the corresponding experimental results at different welding conditions and the results were found to be in good agreement.

Furthermore, it was observed that the arc root dimensions increase with the instantaneous welding current and voltage. Further, at an approximately constant instantaneous current, a reduction in the arc root dimensions is noted with the arc interaction. Next it is observed that the arc interaction has a significant influence on the droplet transfer direction. The detached droplet follows the axis of the arc at the time of detachment irrespective of the direction of the present arc axis.

2.3 Statistical predictive models

Empirical prediction models based on multiple regression analysis have become a useful tool in estimating several weld joint characteristics as function of welding conditions. Chande[13] proposed three different relations of electrode melting rate for DCEP, DCEN and AC single wire SAW processes as function of welding current, electrode diameter and electrode extension as follows:

$$\begin{aligned} MR_{EP} &= [0.01037 * I] + [2.2426 * 10^{-6} * (I^2 \ell^{el} / \phi^2)] - 0.462 \\ MR_{EN} &= [0.0161781 * I] + [2.087 * 10^{-6} * (I^2 \ell^{el} / \phi^2)] - 0.643 \\ MR_{AC} &= [0.015231 * I] + [1.6882 * 10^{-6} * (I^2 \ell^{el} / \phi^2)] - 2.396 \end{aligned} \quad (3\text{-}5)$$

where MR_{EP}, MR_{EN} and MR_{AC} refer to melting rate (kg/h) during DCEP, DCEN and AC modes, respectively, I is the welding current (A), ϕ is the electrode diameter (mm), and ℓ^{el} is the electrode extension (mm). In eqs. (3)-(5), the coefficients of the resistance heating term ($I^2 \ell^{el} / \phi^2$) is smaller than that of the arc heating term (I) indicating the former to be less dominant. Furthermore, the coefficient of the arc heating term in DCEN is higher than in the case of DCEP depicting that the electrode melting due to arc heating is of greater significance in DCEN. The effect of arc heating on the electrode melting rate during AC is intermediate between DCEP and DCEN. Chandel et al. [32] also performed similar studies to realize the influence of welding conditions on the flux consumption rate during SAW of ASTM A36 mild steel plate of 19 mm thickness.

Murugan et al.[5] presented the weld bead dimensions and dilution as function of welding conditions in single wire SAW process as follows:

$$\begin{aligned} d &= 2.6107 + 0.4536 * w_f - 0.2964 * v - 0.1307 * \ell^{el} \\ &\quad - 0.1242 * w_f * v \\ h &= 2.6268 - 0.1375 * V + 0.2417 * w_f - 0.3188 * v \\ &\quad + 0.0969 * V * v + 0.1527 * v^2 \\ w &= 37.857 - 1.933 * V + 0.775 * w_f - 4.542 * v \\ &\quad - 0.8268 * w_f^2 \\ D &= 43.821 + 2.358 * w_f - 1.0625 * V - 1.83 * V * v \end{aligned} \quad (8\text{-}11)$$

where w, d, h, and D refer to the weld width (mm), penetration (mm), reinforcement height (mm) and % dilution, respectively. The terms V, w_f, v and ℓ^{el} refer to welding voltage (V), wire feed rate (mm/s), welding speed (mm/s) and electrode extension (mm), respectively. Equations (8), (9) and (11) indicate that the interaction of the welding conditions also influences the weld bead dimensions and percent dilution. A similar study was also reported by Gunraj et al.[6] on single wire SAW process of IS 2062 carbon steels and Kim et al.[36] in case o fGMAW process.

Tusek et al. [11] developed prediction models of electrode melting rates as function of welding conditions in twin-wire SAW process as:

$$\begin{aligned} MR_{EP} &= 0.02393 * I + 3.6093 * 10^{-6} * (I^2 \ell^{el} / \phi^2) - 0.739 \\ MR_{EN} &= 0.03193 * I + 3.0984 * 10^{-6} (I^2 \ell^{el} / \phi^2) - 0.876 \end{aligned} \quad (12\text{-}13)$$

Equations (12) and (13) indicate that the melting of electrodes consumes greater arc energy in the case of DCEN polarity and thus higher welding speeds can be used. Tusek et al.[12] also proposed empirical relations to predict the rate of melting in three-wire SAW process for both DCEP and DCEN polarity as

$$\begin{aligned} MR_{EP} &= 0.0474 * I + 4.0168 * 10^{-6} * (I^2 \ell^{el} / \phi^2) - 1.996 \\ MR_{EN} &= 0.0571 * I + 3.693 * 10^{-6} * (I^2 \ell^{el} / \phi^2) - 1.219 \end{aligned} \quad (14\text{-}15)$$

A comparison of equations (12) to (15) indicates an increase in both the resistance and the arc heating with the increase in number of welding wires for a given welding current. Sharma et al. [33] estimated the melting rate in twin-wire SAW process for both DCEN and DCEP with equal and different wire diameters. Sharma et al.[34] also proposed empirical relations for the estimation of the rate of flux consumption in twin-wire SAW process. Kiran et al.[26] designed the experiments using central composite rotatable design to study the influence of leading and trailing wire process parameters on the weld quality in SAW-T process. Furthermore, second order response surface models of the weld bead dimensions and the weld mechanical properties as a function of process parameters are developed.

3. Conclusions

A brief review of the experimental studies on the single wire and multi-wire SAW processes is the focus of the present paper. The influence of various process parameters involved in the SAW processes on the weld bead dimensions, metallurgical phases and mechanical properties are discussed. Some of the salient points in the present review are summarized as below.

- Increase in welding current enhances the melting rate of the electrode and flux, weld width, penetration and reinforcement height. For a given welding current electrode melting rate and flux melting rate is the highest in DCEN, followed by AC and DCEP.
- Decrease in arc voltage has increased the electrode melting rate and reinforcement height but decreased the flux melting rate and the weld width while showed no effect on the weld penetration.
- For a given current, increase in the electrode diameter decrease the electrode melting rate, reinforcement height and weld penetration, while increase the weld width. On the other hand, increase in the electrode extension enhance the electrode melting rate and weld width with smaller penetration.
- The weld width, penetration and reinforcement height increased inversely with the welding speed.
- Higher electrode melting rate in the case of the twin-wire SAW process is observed in comparison to the single wire SAW process for a given welding current.
- Increase in either trailing wire current or the leading wire current results in higher weld bead dimensions in SAW-T process. At smaller welding current and shorter electrode extension length, increase in the inclination angle of the trailing electrode wire has decreased the weld penetration in SAW-T process.
- The final weld microstructure in submerged arc weldment depend on the cooling rate from 800 to 500℃ ($\Delta T_{8/5}$), prior austenite grain size, distribution of non-metallic inclusions and chemical composition of the weld. In particular, $\Delta T_{8/5}$ is envisaged to be an effective indicator of the extent of austenite to ferrite transformation in HSLA welds. The weld metal tensile strength and toughness would improve with greater volume fraction of acicular ferrite due to its fine grains, interlocking nature and high angle boundaries that could act as obstacles to cleavage crack propagation.
- With the increase in heat input, the Charpy impact toughness has reached a peak value and then decreased with further increase in the heat input. Increase in welding speed has increased the hardness and Charpy impact toughness values in both HAZ and weld metal.
- In SAW-T process, the increase in leading wire current or trailing wire current pulses enhance allotriomorphic ferrite phase and reduces acicular ferrite. On the other hand, allotriomorphic ferrite phase reduces with increase in trailing wire negative cycle time for a given frequency or welding speed (v), while acicular ferrite increases.
- The leading and trailing wire currents have negative influence on the weld strength and toughness while the trailing wire negative pulse time and welding speed have positive

influence.

- Arc interaction has a significant influence on the stability of the arc, and the leading and trailing arc root dimensions. The physical models for the prediction of arc center displacement are developed and validated with the corresponding experimental values at different welding conditions. Furthermore, significant influence of the arc interaction on the molten droplet transfer direction is reported.

Acknowledgements

The authors gratefully acknowledge the support of the Brain Korea 21 plus project, Korean Ministry of Knowledge Economy (No.2013-10040108) and Mid-career 363 Researcher Program through NRF (2013-015605).

References

1. G. Almqvist : Submerged arc welding, The Welding Institute, Cambridge, (1978)
2. M. H. Robinson : Observations on electrode melting rates during submerged arc welding, Welding Journal, **40-11** (1961), 503s-515s
3. R. S. Chandel : Mathematical modeling of melting rates for submerged arc welding, Welding Journal, **68-5** (1987), 135s-140s
4. B. G. Renwick and B. M. Patchett : Operating characteristics of the submerged arc welding process, Welding Journal, **55-3** (1976), 69s-76s
5. N. Murugan, R. S. Parmar and S. K. Sud : Effect of submerged arc process variables on dilution and bead geometry in single wire surfacing, Journal of Materials Processing Technology, **37-1** (1993), 767-780
6. V. Gunaraj and N. Murugan : Application of response surface methodology for predicting weld bead quality in submerged arc welding of pipes, Journal of materials processing technology, **88-11** (1999), 266-275
7. T. Ueyama, T. Ohnawa, M. Tanaka and K. Nakata: Effects of torch configuration and welding current on weld bead formation in high speed tandem pulsed gas metal arc welding of steel sheets, Science and Technology of Welding and Joining, **10-7** (2005), 750-759
8. G. D. Uttrachi : Multiple electrode systems for submerged arc welding, Welding Journal, **78-5** (1978), 15-22
9. G. D. Uttrachi and J. E. Messina : Three wire submerged arc welding of line pipe, Welding Journal, **47-6** (1968), 475-481
10. Lincoln electric company : Waveform control technology power wave AC/DC submerged arc, Lincolnelectric. com, last visited on 25/8/2008
11. J. Tusek : Mathematical modeling of melting rate in twin-wire welding, Journal of Materials Processing Technology, **100-12** (2000), 250-256
12. J. Tusek : Mathematical modeling of melting rate in arc welding with a triple wire Electrode, Journal of Materials Processing Technology, **146-2** (2004), 415-423
13. P. J. Konkol and G. F. Koons : Optimization of parameters for two-wire DC-AC submerged arc welding, AWS Welding Journal, **78-12** (1978), 367s-374s
14. O. Grong and D. K. Matlock : Microstructural development in mild and low alloy steel weld metals, International Metals Reviews, **31-1** (1986), 27-48
15. S. S. Babu : The mechanism of acicular ferrite in weld deposits, Current Opinion in Solid State and Materials Science, **8-3** (2004), 267-278
16. R. A. Farrar and P. L. Harrison : Acicular ferrite in carbon-manganese weld metals: an overview, Journal of Materials Science, **22-11** (1987), 3812-3820
17. H. Motohashi, N. Hagiwara and T. Masuda: Tensile properties and microstructure of weld metal in MAG welded X80 pipeline steel, Welding International, **19-12** (2005), 100-108
18. H. K. D. H. Bhadeshia, D. J. C. MacKay and L. E. Svensson : The impact toughness of C-Mn steel arc welds- A Bayesian neural network analysis, Material Science and Technology, **11-10** (1995), 1046-1051
19. K. Prasad and D. K. Dwivedi : Some investigations on microstructure and mechanical properties of submerged arc welded HSLA steel joints, International Journal of Advanced Manufacturing Technology, **36-5** (2008), 475-483
20. S. H. Hashemi, D. Mohammadyani, M. Pouranvari and S. M. Mousavizadeh : On the relation of microstructure and impact toughness characteristics of DSAW steel of grade API X70, Fatigue and Fracture of Engineering Materials and structures, **32-1** (2008), 33-40
21. A. Hall : The effect of welding speed on the properties of ASME SA516 Grade 70 steel, M.S thesis, University of Saskatchewan, Saskatoon, (2010)
22. H. Farhat : Effects of multiple wires and welding speed on the microstructures and properties of submerged arc welded X80 steel, Ph.D thesis, University of Saskatchewan, Saskatoon, 2007
23. D. M. Viano, N. U. Ahmed and G. O. Schumann: Influence of heat input and travel speed on microstructure and mechanical properties of double tandem submerged arc high strength low alloy steel weldments, Science and Technology of Welding and Joining, **5-1** (2000), 26-34
24. S. Moeinifar, A. H. Kokabi and H. R. M. Hosseini: Role of tandem submerged arc welding thermal cycles on properties of the heat affected zone in X80 microalloyed pipe line steel, Journal of Materials Processing Technology, **211-9** (2011), 368-375
25. S. Moeinifar, A. H. Kokabi and H. R. M. Hosseini:

Effect of tanden submerged arc welding process and parameters of Gleeble simulator thermal cycles on properties of the intercrtically reheated heat affected zone, Materials and Design, **32-7** (2011), 869-876
26. D. V. Kiran, B. Basu and A. De : Influence of process variables on weld bead quality in two wire tandem submerged arc welding of HSLA steel, Journal of Materials Processing Technology, **212-10** (2012), 2041-2050
27. D. V. Kiran, B. Basu, A. K. Shah, S. Mishra and A. De : Probing influence of welding current on weld quality in two wire tandem submerged arc welding of HSLA steel, Science and Technology of Welding and Joining, **15-2** (2010), 111-116
28. K. Prasad and D. K .Dwivedi : Microstructure and tensile properties of submerged arc welded 1.25 Cr-0.5 Mo steel joints, Materials and Manufacturing Processes, **23** (2008), 463-468
29. D. V. Kiran, S. A. Alam and A. De : Development of process maps in two wire tandem submerged arc welding process of HSLA steel, **22-4** (2013), 988-994
30. D. V. Kiran, D. W. Cho, W. H. Song and S. J . Na : Arc behavior in two wire tandem submerged arc welding, Journal of Materials Processing Technology, **214-8** (2014), 1546-1556]
31. M. F. Mruczek : Cold wire feed submerged arc welding, Concurrent Technologies Corporation research report, Concurrent Technologies Corporation, Johnstown, (2006)
32. R. S. Chandel : The effect of process variables on the flux consumption in submerged arc welding, Materials and Manufacturing Process, **13-2** (1998), 181-188
33. A. Sharma, N. Arora and K. M. Bhanu : A practical approach towards mathematical modeling of deposition rate during twin-wire submerged arc welding, International Journal of Advanced Manufacturing Technology, 3**6-5** (2006), 463-474
34. A. Sharma, N. Arora and K. M. Bhanu : Mathematical modeling of flux consumption during twin-wire welding, International Journal of Advanced Manufacturing Technology, **38-11** (2008), 1114-1124
35. S. H. Lee and S. J. Na : A study on the arc characteristics and weld pool analysis of GHTAW under the space environment, Journal of KWJS, **28-4** (2010), 67-72
36. I. S. Kim, W. H. Kwon and C. E. Park : The effects of welding process parameters on weld bead width in GMAW processes, Journal of KWS, **14-4** (1996), 33-42

Degala Ventaka Kiran received the B.E. degree in mechanical engineering from Andhra University, Visakhapatnam, India, in 2005, M.Tech degree in mechanical and industrial engineering from IIT Roorkee, Roorkee, India in 2007 and the Ph.D. degree in mechanical enginee- ring from IIT Bombay, Mumbai, India in 2012.

He is a Post doctoral researcher with the Advanced Laser, Plasma and Hybrid Applications Lab, Korea Advanced Institute of Science and Technology, Daejeon, Korea. His current research interests include Weldig Science and Technology, numerical analysis of heat transfer and fluid flow, residual stress and deformation in fusion welding processes, experimental stress analysis, and statistical modeling and optimization.

Suck-Joo Na graduated from Seoul National University for B.Sc. and Korea Advanced Institute of Science and Technology for M.Sc. in Mechanical Engineering, and has got his Dr.-Ing. degree from the Welding and Joining Institute of TU Braunschweig, Germany.

Professor Na is working at KAIST, Korea for more than 30 years, educating and researching in the analysis, optimization and automation of welding processes and laser materials processing. Professor Na is one of the leading scientists in the field of process simulation of arc and laser beam welding, most notably of laser hybrid welding, in which he links his expertise of arc physics and multiple reflections in the keyhole with that of weld pool dynamics during arc and laser welding. He has published 236 research papers in SCI and Korean domestic journals, and presented more than 230 papers at international and domestic conferences.

Professor Na has been awarded various prizes from Korean Welding and Joining Society (KWJS), American Welding Society (AWS) such as excellent scientific research award, best paper award and Charles H. Jennings Memorial Award. He was elected as the fellow of AWS in 2005, as the member of the National Academy of Engineering of Korea in 2007 and[as the fellow of the Korean Academy of Science and Tech- nology in 2008. Recently he was selected as the FiDiPro Professor to establish a digital welding research group at VTT in Finland from 2014 to 2016.

After serving as a member of the board of directors of KWJS, Professor Na was the president of KWJS from 2007 to 2008, a member of Technical Management Board of IIW from 2010 to 2012 and is now serving as the president of Asian Welding Federation.